Plane-Wave Diffraction by a Slit in a Thin Material Screen

Takashi Nagasaka and Kazuya Kobayashi

Abstract – H-polarized plane-wave diffraction by a slit in a material screen is analyzed using the Wiener–Hopf technique and generalized boundary conditions. Exact and high-frequency asymptotic solutions are obtained. The scattered field is evaluated asymptotically based on the saddle-point method, and a far-field expression is derived. Numerical examples on the far-field intensity are presented and the scattering characteristics of the slit are discussed.

1. Introduction

Analysis of the scattering by a slit in a material screen is an important topic in diffraction theory and relevant for many engineering applications. Slit structures provide simple diffraction problems that describe the effect of multiply diffracted fields. A number of scientists have analyzed slit-diffraction problems using various analytical and numerical methods. In our pervious work [1, 2], we have analyzed the plane-wave diffraction by a thin material strip using the Wiener–Hopf technique [3] and approximate boundary conditions [4], and obtained a rigorous, high-frequency solution. In this article, we shall consider a slit in an infinitely thin material screen and analyze the H-polarized plane-wave diffraction with the aid of the Wiener–Hopf technique by following a procedure similar to that used in [1, 2].

After introducing the Fourier transform of the scattered field and applying generalized boundary conditions [5] in the transform domain, the problem is formulated in terms of the simultaneous Wiener–Hopf equations, which are solved exactly via the factorization and decomposition procedure. However, the solution is formal because branch-cut integrals with unknown integrands are involved. We shall further use a rigorous asymptotic method to derive a high-frequency solution to the Wiener–Hopf equations. Our final solution is valid for the case where the slit width is large in comparison to the wavelength. The scattered field is evaluated asymptotically by taking the inverse Fourier transform and applying the saddle-point method. Numerical examples are presented for various physical parameters, and scattering characteristics of the slit are discussed.

The time factor is assumed to be $e^{-i\omega t}$ and is suppressed throughout this article.

Manuscript received 27 December 2021.

Takashi Nagasaka and Kazuya Kobayashi are with the Department of Electrical, Electronic, and Communication Engineering, Chuo University, 1-13-27 Kasuga, Bunkyo-ku, Tokyo 112-8551, Japan; e-mail: nagasaka@elect.chuo-u.ac.jp, kazuya@tamacc.chuo-u.ac.jp.

2. Formulation of the Problem

We consider the H-polarized plane-wave diffraction by a slit in a thin material screen as shown in Figure 1, where ε_r and μ_r are the relative permittivity and permeability of the material, respectively.

Since the thickness of the material screen is small compared with the wavelength, it can be replaced by a screen of zero thickness satisfying the generalized boundary conditions [5]. On the material surface, the total field satisfies the generalized boundary conditions given by

$$\frac{1}{2}\left[E_z^t(+0,z)+E_z^t(-0,z)\right]=R_{\mathrm{T}}\left[H_y^t(+0,z)-H_y^t(-0,z)\right] \tag{1}$$

$$\frac{1}{2}\left[H_y^t(+0,z)+H_y^t(-0,z)\right]=S_{\mathrm{T}}\left[E_z^t(+0,z)-E_z^t(-0,z)\right] \tag{2}$$

where

$$R_{\mathrm{T}}=\frac{1}{2}iZ_0\left(\mu_r^{1/2}/\varepsilon_r^{1/2}\right)\cot\left[kb(\varepsilon_r\mu_r)^{1/2}/2\right] \tag{3}$$

$$S_{\mathrm{T}}=\frac{1}{2}iY_0\left(\varepsilon_r^{1/2}/\mu_r^{1/2}\right)\cot\left[kb(\varepsilon_r\mu_r)^{1/2}/2\right] \tag{4}$$

with Z_0 and Y_0 being the intrinsic impedance and admittance of free space, respectively. Note that (1) and (2) are valid for $kb \ll 1$ and $|\varepsilon_r\mu_r| \gg 1$.

Taking into account that the original material screen of finite thickness has been replaced by an infinitely thin screen, we define the total magnetic field $\phi^t(x,z)$ as

$$\begin{aligned}\phi^t(x,z)&=\phi^i(x,z)+R_a\phi^i(-x,z)+\phi(x,z), \quad x>0\\ &=T_a\phi^i(x,z)+\phi(x,z), \quad x<0\end{aligned} \tag{5}$$

where $\phi^i(x,z)$ is the incident field given by

$$\phi^i(x,z)=e^{-ik(x\sin\theta_0+z\cos\theta_0)}, \qquad k=\omega(\varepsilon_0\mu_0)^{1/2} \tag{6}$$

for $0<\theta_0<\pi/2$. In (5), $R_a\phi^i(-x,z)$ and $T_a\phi^i(x,z)$ denote the reflected and transmitted fields from the infinitely thin screen, respectively, and $\phi(x,z)$ is the unknown scattered field satisfying the two-dimensional Helmholtz equation. The reflection coefficient R_a and the transmission coefficient T_a are defined as follows:

$$T_a+R_a=-(Y_0-2S_{\mathrm{T}}\sin\theta_0)/(Y_0+2S_{\mathrm{T}}\sin\theta_0) \tag{7}$$

$$T_a-R_a=(2Y_0R_{\mathrm{T}}-\sin\theta_0)/(2Y_0R_{\mathrm{T}}+\sin\theta_0) \tag{8}$$

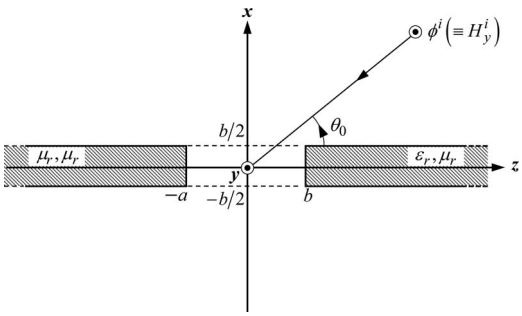

Figure 1. Geometry of the problem.

In the following, we shall assume that the medium is slightly loss, as in $k = k_1 + ik_2$ with $0 < k_2 \ll k_1$.

We define the Fourier transform of the unknown scattered field $\phi(x,z)$ with respect to z as

$$\Phi(x,\alpha) = (2\pi)^{-1/2} \int_{-\infty}^{\infty} \phi(x,z) e^{i\alpha z} dz \tag{9}$$

where $\alpha(\equiv \sigma + i\tau)$. Then we see with the aid of the radiation condition that $\Phi(x,\alpha)$ is regular in the strip $|\tau| < k_2 \cos\theta_0$ of the complex α-plane. Introducing the Fourier integrals as

$$\Phi_{\pm}(x,\alpha) = \pm(2\pi)^{-1/2} \int_{\pm a}^{\pm\infty} \phi(x,z) e^{i\alpha(z\mp a)} dz \tag{10}$$

$$\Phi_1(x,\alpha) = (2\pi)^{-1/2} \int_{-a}^{a} \phi(x,z) e^{i\alpha z} dz \tag{11}$$

it follows that $\Phi_+(x,\alpha)$ and $\Phi_-(x,\alpha)$ are regular in the half-planes $\tau > -k_2 \cos\theta_0$ and $\tau < k_2 \cos\theta_0$, respectively, and $\Phi_1(x,\alpha)$ is an entire function.

Taking the Fourier transform of the Helmholtz equation and using the radiation condition, we find that

$$\Phi(x,\alpha) = \tilde{\Phi}(\alpha) e^{-\gamma|x|} \tag{12}$$

where $\gamma = (\alpha^2 - k^2)^{1/2}$ with $\mathrm{Re}\gamma > 0$ and

$$\tilde{\Phi}(\alpha) = -\frac{1}{2\gamma}\left[U_{(+)}(\alpha) e^{i\alpha a} + U_-(\alpha) e^{-i\alpha a}\right] \pm \frac{1}{2}\left[V_{(+)}(\alpha) e^{i\alpha a} + V_-(\alpha) e^{-i\alpha a}\right], \quad x \gtrless 0 \tag{13}$$

In (13), various quantities are defined as

$$\left.\begin{matrix} U_{(+)}(\alpha) \\ U_-(\alpha) \end{matrix}\right\} = J'_{\pm}(\alpha) \mp \frac{A_{1,2}}{\alpha - k\cos\theta_0} \tag{14}$$

$$\left.\begin{matrix} V_{(+)}(\alpha) \\ V_-(\alpha) \end{matrix}\right\} = J_{\pm}(\alpha) \mp \frac{B_{1,2}}{\alpha - k\cos\theta_0} \tag{15}$$

where

$$J'_{\pm}(\alpha) = \frac{d}{dx}\left[\Phi_{\pm}(+0,\alpha) - \Phi_{\pm}(-0,\alpha)\right] \tag{16}$$

$$J_{\pm}(\alpha) = \Phi_{\pm}(+0,\alpha) - \Phi_{\pm}(-0,\alpha) \tag{17}$$

$$A_{1,2} = (2\pi)^{-1/2} k \sin\theta_0 (T_a + R_a - 1) e^{\mp ika\cos\theta_0} \tag{18}$$

$$B_{1,2} = i(2\pi)^{-1/2} (T_a - R_a - 1) e^{\mp ika\cos\theta_0} \tag{19}$$

In (16) and (17), $J'_{\pm}(\alpha)$ and $J_{\pm}(\alpha)$ denote the Fourier transforms of the unknown magnetic and electric surface currents on the material, respectively. Equation (12) is the scattered-field representation in the Fourier-transform domain. Taking into account the boundary conditions, we obtain

$$-M(\alpha)\Phi_1^t(0,\alpha) = U_{(+)}(\alpha) e^{i\alpha a} + U_-(\alpha) e^{-i\alpha a} \tag{20}$$

$$-K(\alpha)\Phi_1^{t'}(0,\alpha) = V_{(+)}(\alpha) e^{i\alpha a} + V_-(\alpha) e^{-i\alpha a} \tag{21}$$

where

$$M(\alpha) = 2\gamma k Y_0 / (kY_0 + i2S_{\mathrm{T}}\gamma) \tag{22}$$

$$K(\alpha) = 2/(\gamma - i2kY_0 R_{\mathrm{T}}) \tag{23}$$

and $M(\alpha)$ and $K(\alpha)$ are the kernel functions, and $\Phi_1^t(0,\alpha)$ and $\Phi_1^{t'}(0,\alpha)$ are entire functions. Equations (20) and (21) are the Wiener–Hopf equations satisfied by the unknown spectral functions.

3. Exact and Asymptotic Solutions

The kernel functions $M(a)$ and $K(\alpha)$ in (22) and (23) can be factorized as

$$M(\alpha) = M_+(\alpha) M_-(\alpha), \quad K(\alpha) = K_+(\alpha) K_-(\alpha) \tag{24}$$

where

$$M_{\pm}(\alpha) = 2^{1/2} e^{-i\pi/4} (k \pm \alpha)^{1/2} \Big/ N_{1\pm}(\alpha) \tag{25}$$

$$K_{\pm}(\alpha) = e^{i\pi/4} \Big/ \left[(kY_0 R_{\mathrm{T}})^{1/2} N_{2\pm}(\alpha)\right] \tag{26}$$

with

$$N_{n\pm}(\alpha) = \left(1 + \delta_n^{-1}\right)^{1/2} \left\{1 + \alpha^2 / \left[k^2\left(\delta_n^2 - 1\right)\right]\right\}^{1/4} \cdot \exp\left\{ -\frac{\delta_n}{\pi} \int_{\pi/2}^{\arccos(\pm\alpha/k)} \frac{t\cos t}{\sin^2 t - \delta_n^2} dt \pm \frac{i}{2\pi} \ln\left[\delta_n + \left(\delta_n^2 - 1\right)^{1/2}\right] \ln\left[\frac{ik\left(\delta_n^2 - 1\right)^{1/2} + \alpha}{ik\left(\delta_n^2 - 1\right)^{1/2} - \alpha}\right] \right\} \tag{27}$$

$$\delta_1 = Y_0/(2S_{\mathrm{T}}), \quad \delta_2 = 2Y_0 R_{\mathrm{T}} \tag{28}$$

We multiply both sides of (20) by $e^{\mp i\alpha a}/M_{\pm}(\alpha)$ and apply the decomposition procedure with the aid of the edge condition [4]. This leads to

$$U_{(+)}^{s,d}(\alpha) = M_+(\alpha)\left[\frac{-A_1}{M_+(k\cos\theta_0)(\alpha - k\cos\theta_0)} \mp \frac{A_2}{M_-(k\cos\theta_0)(\alpha + k\cos\theta_0)} \pm u_{s,d}(\alpha)\right] \tag{29}$$

where

$$U_{(+)}^{s,d}(\alpha) = U_{(+)}(\alpha) \pm U_-(-\alpha) \tag{30}$$

$$u_{s,d}(\alpha) = \frac{1}{\pi i}\int_k^{k+i\infty} \frac{F_+(\beta)U_{(+)}^{s,d}(\beta)}{(\beta - k)^{1/2}(\beta + \alpha)} e^{2i\beta a} d\beta \tag{31}$$

with

$$F_+(\beta) = M_+(\beta)\Big/\left[2(\beta + k)^{1/2}\right] \tag{32}$$

Equation (29) is the exact solution to the Wiener–Hopf equation (20), but it is formal because the branch-cut integrals with the unknown integrands $u_{s,d}(\alpha)$ defined by (31) are involved.

Applying the asymptotic method established in our previous work [1, 2] to the branch-cut integrals in (31), we derive an explicit asymptotic solution to the Wiener–Hopf equation (20) with the result that

$$\left.\begin{matrix} U_{(+)}(\alpha) \\ U_-(\alpha) \end{matrix}\right\} \sim M_\pm(\alpha)\left[\frac{\mp A_{1,2}}{M_\pm(k\cos\theta_0)(\alpha - k\cos\theta_0)} + A_{2,1}\eta_{f1,f2}(\pm\alpha) + \sum_{n=0}^{N} \frac{f_n^{us} \mp f_n^{ud}}{2}\xi_{0n}^f(\pm\alpha)\right] \tag{33}$$

as $ka \to \infty$, where N denotes the truncation number of the infinite asymptotic series and

$$f_n^{us,ud} = \frac{1}{n!}\frac{d^n J_+^{'s,d}(\alpha)}{d\alpha^n}\bigg|_{\alpha=k} \tag{34}$$

$$\xi_{0n}^f(\alpha) = \frac{e^{2ika}}{\pi i}\left(\frac{i}{2a}\right)^{n-1/2}\Gamma_1^f\left[\frac{1}{2} + n, -2i(\alpha + k)a\right] \tag{35}$$

$$\eta_{f1,f2}(\alpha) = \frac{\xi_{00}^f(\alpha) - \xi_{00}^f(\pm k\cos\theta_0)}{\alpha \mp k\cos\theta_0} \tag{36}$$

with

$$J_+^{'s,d}(\alpha) = J_+'(\alpha) \pm J_-'(-\alpha) \tag{37}$$

$$\Gamma_m^f(u,v) = \int_0^\infty \frac{t^{u-1}e^{-t}}{(t+v)^m} F_+[k + it/(2a)]d\beta \tag{38}$$

The unknowns $f_n^{us,ud}$ in (33) are determined by following a procedure similar to that used in [1, 2], but the details are omitted here. Equation (21) can be also solved in a similar manner.

4. Scattered Far Field and Numerical Examples

The scattered field in real space is obtained by taking the inverse Fourier transform of (12). We introduce the polar coordinates $x = \rho\sin\theta$ and $z = \rho\cos\theta$ for $-\pi < \theta < \pi$ and apply the saddle-point method of integration. Then it is found that $\phi(x,z)$ has the asymptotic expansion

$$\phi(\rho,\theta) \sim \tilde{\Phi}(-k\cos\theta)k\sin|\theta|(k\rho)^{-1/2}e^{i(k\rho - \pi/4)} \tag{39}$$

as $k\rho \to \infty$. Equation (39) is uniformly valid for arbitrary incidence and observation angles.

We shall now present numerical examples of the scattered far field and discuss the scattering characteristics. The normalized far-field intensity is introduced as follows:

$$|\phi(\rho,\theta)|[\text{dB}] = 20\log_{10}\left[\frac{\lim_{\rho\to\infty}\left|(k\rho)^{1/2}\phi(\rho,\theta)\right|}{\max_{|\theta|\le\pi}\lim_{\rho\to\infty}\left|(k\rho)^{1/2}\phi(\rho,\theta)\right|}\right] \tag{40}$$

Figure 2 shows numerical examples of the scattered far-field intensity versus the observation angle θ where the slit width is $2a = 10\lambda$ and the material thickness is $b = 0.01\lambda$, 0.02λ, and 0.03λ. We have fixed the incidence angle as $\theta_0 = 60°$ and the truncation number of the asymptotic series (33) as $N = 0$. We can verify that the choice $N = 0$ gives sufficient accuracy. As an example of existing lossy materials, we have chosen Fe_3O_4 powder with $\varepsilon_r = 7.479 + i0.368$ and $\mu_r = 2.538 + i1.706$ in numerical computation [6]. Note from the figure that the field intensity shows noticeable peaks along the reflection boundary $\theta = 120°$ and the incidence shadow boundary $\theta = -120°$, as expected. Comparing the far-field characteristics for different thicknesses b, the results exhibit close features over the range $-180° < \theta < 0°$, whereas they show some differences within the range $0° < \theta < 180°$.

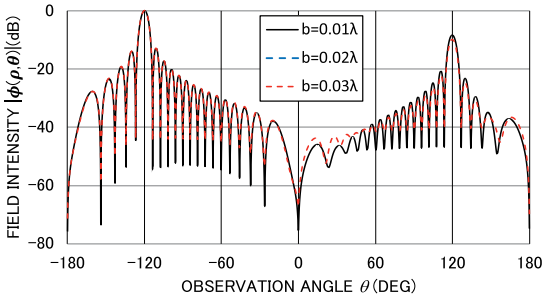

Figure 2. Scattered far field $|\phi(\rho,\theta)|$[dB] for $\theta_0 = 60°$, $N = 0$, $2a = 10\lambda$, $\varepsilon_r = 7.479 + i0.368$, and $\mu_r = 2.538 + i1.706$.

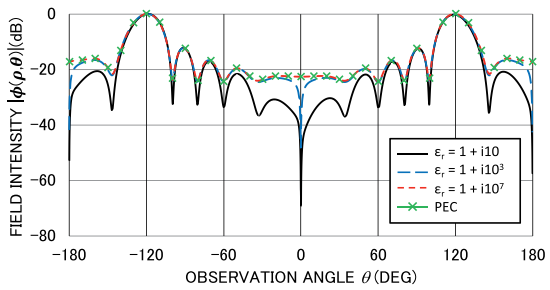

Figure 3. Scattered far field $|\phi(\rho,\theta)|$[dB] for $\theta_0 = 60°$, $N = 0$, $2a = 3\lambda$, $b = 0.01\lambda$, and $\mu_r = 1$.

Figure 3 shows a comparison of the results for different imaginary parts of ε_r, where the slit width and the material thickness are fixed at $2a = 3\lambda$ and $b = 0.01\lambda$, respectively, and $\mu_r = 1$. From the figure, we note that with increasing $\mathrm{Im}\varepsilon_r$, the results approach those for a slit in an infinitely thin perfect electric conductor [7].

5. Conclusions

We have solved H-polarized plane-wave diffraction by a slit in a thin material screen using the Wiener–Hopf technique and generalized boundary conditions. Using rigorous asymptotics, a high-frequency solution for large slit width has been obtained. Numerical examples are presented for various physical parameters, and the far-field scattering characteristics of the slit have been discussed in detail.

6. References

1. T. Nagasaka and K. Kobayashi, "Wiener-Hopf Analysis of the Plane Wave Diffraction by a Thin Material Strip," *IEICE Transactions on Electronics*, **E100-C**, 1, January 2017, pp.11-19.
2. T. Nagasaka and K. Kobayashi, "Wiener-Hopf Analysis of the Plane Wave Diffraction by a Thin Material Strip: The Case of E Polarization," *IEICE Transactions on Electronics*, **E101-C**, 1, January 2018, pp.12-19.
3. B. Noble, *Methods Based on the Wiener-Hopf Technique for the Solution of Partial Differential Equations*, London, Pergamon, 1958.
4. T. B. A. Senior and J. L. Volakis, *Approximate Boundary Conditions in Electromagnetics*, London, The Institution of Electrical Engineers, 1995.
5. E. H. Bleszynski, M. K. Bleszynski, and T. Jaroszewicz, "Surface-Integral Equations for Electromagnetic Scattering From Impenetrable and Penetrable Sheets," *IEEE Antennas and Propagation Magazine*, **35**, 6, December 1993, pp. 14-25.
6. M. Hotta, M. Hayashi, and K. Nagata, "High Temperature Measurement of Complex Permittivity and Permeability of Fe_3O_4 Powders in the Frequency Range of 0.2 to 13.5 GHz," *ISIJ International*, **51**, 3, March 2011, pp. 491-497.
7. S. R. Seshadri, "High-Frequency Diffraction of Plane Waves by an Infinite Slit I & II," *Proceedings of the Indian National Science Academy*, **25**, 6A, November 1959, pp. 301-336.